American Mineralogist, Volume 83, pages 1030–1036, 1998

Volume measurements of zoisite at simultaneously elevated pressure and temperature

A.R. PAWLEY,[1,*] N.J. CHINNERY,[1] AND S.M. CLARK[2]

[1]Department of Earth Sciences, University of Manchester, Oxford Road, Manchester M13 9PL, U.K.
[2]Daresbury Laboratory, Daresbury, Warrington, Cheshire WA4 4AD, U.K.

ABSTRACT

Unit-cell parameters of zoisite, $Ca_2Al_3Si_3O_{12}(OH)$, have been measured at simultaneously high pressures and temperatures (up to 6.1 GPa and 800 °C) in a Walker-style multi-anvil apparatus at the synchrotron radiation source at Daresbury Laboratory, U.K. Measurements were made in a series of heating cycles at increasing loads. Sample pressure, measured using an internal NaCl standard, increased during heating. Cell parameters vary smoothly with pressure and temperature; individual expansivities and compressibilities vary in the order $c > b > a$. Isothermal bulk moduli were calculated from the volumes measured at 30, 200, 400, 600, and 800 °C by fitting the Murnaghan equation of state to each isothermal data set. This assumes $K' = 4$. Ambient-pressure volumes calculated from previous measurements of thermal expansivity of zoisite were included in the Murnaghan fits. A linear fit of the bulk moduli with temperature gave values for the bulk modulus at 298 K, $K_{298} = 125(3)$ GPa, and its variation with temperature, $\partial K_T/\partial T = -0.029(6)$ GPa K^{-1}. K_{298} is slightly higher than the recent value for a single crystal in a diamond-anvil cell, indicating a lower maximum pressure stability of zoisite than would be calculated using that value. Our data allow zoisite volumes to be calculated at *P-T* conditions relevant to the Earth and show that, in a typical subduction zone, zoisite becomes more dense as subduction proceeds, helping to stabilize it to high pressures.

INTRODUCTION

Knowledge of the stabilities of hydrous minerals in the Earth is an important requirement for understanding mantle processes and properties. For example, hydrous magmas can result from dehydration-melting reactions in the mantle and may lead to explosive volcanism; earthquakes can be triggered by dehydration reactions; seismic and rheological properties are affected by the presence of hydrous phases; and the evolution of the Earth's H_2O budget over time depends on the ability of mantle phases to store H_2O. To place constraints on the scope of these processes, the *P-T* positions of reactions in which potentially important high-pressure hydrous phases are involved must be determined.

Some high *P-T* reactions can be investigated directly in phase-equilibrium experiments, but the information thus provided is limited to the compositional system and to the particular *P-T* conditions studied. Extrapolation to relevant mantle compositions and *P-T* conditions then requires the use of thermodynamic data. One of the most important thermodynamic parameters for high *P-T* calculations is the unit-cell volume of a mineral. Its variation with pressure and temperature is described by its equation of state (EOS), with three components: (1) compressibility at ambient temperature, (2) thermal expansivity at ambient pressure, and (3) cross derivative terms describing the effect of pressure on thermal expansivity, equivalent to the effect of temperature on compressibility. For accurate thermodynamic calculations, each component should be measured at relevant *P-T* conditions. However, relevant experimental conditions are often inaccessible, and the third component, which requires volume measurements to be made while the sample is subjected to simultaneous high pressure and high temperature, is often estimated. Fortunately, recent developments of high *P-T* apparatus suitable for in situ experiments now allow such measurements. The usual technique is to use a multi-anvil apparatus and synchrotron radiation (e.g., Meng et al. 1993; Martinez et al. 1996). The multi-anvil apparatus is useful because a wide range of pressures and temperatures can be applied to the sample (e.g., up to 7.9 GPa, 1273 K in the study of Martinez et al. 1996), pressures and temperatures can easily be controlled and measured, large sample volumes permit collection of high quality data, pressure distributions close to hydrostatic can be achieved, and the synchrotron beam has relatively easy access to and from the sample.

This paper describes high *P-T* volume measurements on zoisite, one of several hydrous phases that recent studies have suggested could be stable at considerable depth in the Earth, particularly in subduction zones (e.g., Pawley 1994; Pawley and Wood 1995; Schmidt and Poli 1994; Ulmer and Trommsdorff 1995). Here, oceanic lithosphere generated at mid-ocean ridges is recycled into

* E-mail: alison.pawley@man.ac.uk

0003–004X/98/0910–1030$05.00

the mantle. Hydrothermal alteration close to the mid-ocean ridge gives the crust a high initial H_2O content, and low slab temperatures stabilize hydrous phases to greater depths than in surrounding hotter mantle. Stabilities of these hydrous phases play a major role in controlling subduction zone processes such as dehydration, melting, and magmatism. However, no volume measurement on any hydrous mineral has been previously made at combined high pressure and high temperature. Prior to the recent realization of their potential significance in high-pressure Earth processes, very few measurements even of compressibility at room temperature or thermal expansivity at ambient pressure had been made. Fortunately that situation is changing, and both compressibilities and expansivities of many hydrous phases have been recently measured (e.g., Redfern and Wood 1992; Xu et al. 1994; Faust and Knittle 1994; Comodi and Zanzzi 1996, 1997a, 1997b; Pawley et al. 1995, 1996; Holland et al. 1996). As well as being necessary for calculating phase stabilities, volume measurements of hydrous phases are useful in determining the EOS of H_2O at high pressure and temperature. This is important because volumes of H_2O have been only directly measured at pressures <1 GPa (Burnham et al. 1969). The EOS of H_2O at high pressure can be constrained by measuring the *P-T* positions of dehydration reactions in phase equilibrium experiments (or in situ using synchrotron radiation) and then using known thermodynamic parameters of the solid phases involved to derive the unknown EOS of H_2O (e.g., Johnson and Walker 1993).

Zoisite, $Ca_2Al_3Si_3O_{12}(OH)$, is a common mineral in basaltic rocks metamorphosed in the eclogite and amphibolite facies (e.g., Holland 1979; Franz and Selverstone 1992). Its high-pressure stability has been experimentally determined at ≈6–7 GPa at ≈1000 °C (Schmidt and Poli 1994) indicating that it is capable of transporting H_2O to a depth well beyond the source of subduction zone volcanism. Measurement of the EOS of zoisite at high pressures and temperatures is therefore important for calculating the *P-T* positions of reactions in which it is involved, which will control the fate of the H_2O bound up in zoisite at these depths in the Earth. EOS measurements are also useful for constraining lower *P-T* metamorphic reactions. For example, the monoclinic clinozoisite is another common metamorphic mineral, and so the position of the polymorphic zoisite-clinozoisite reaction could provide a useful indicator of *P-T* conditions attending metamorphism if it were known. However, experiments determining the relative stability of these two minerals produced conflicting results (discussed briefly in Holland et al. 1996; Comodi and Zanazzi 1997a), and it may be only through thermodynamic calculations that it is possible to determine the position of this reaction.

The thermal expansivity of zoisite has been recently measured, using a Guinier camera (Pawley et al. 1996). The compressibility has been measured in two recent studies, with markedly different results. A study using a powdered sample in a diamond-anvil cell, with synchrotron radiation, produced a bulk modulus of 279 GPa (Holland et al. 1996), whereas single-crystal X-ray diffraction (XRD) measurements yielded a bulk modulus of 102 GPa (Comodi and Zanazzi 1997a). We hoped that by remeasuring the compressibility using a different technique we could explain the discrepancy.

Experimental technique

The sample of natural zoisite came from the Moine Schist, Glenurqhart, Scotland (kindly provided by C.M. Graham), and contained 2.3–4.3% of the ferric end-member, $Ca_2Al_2Fe^{3+}Si_3O_{12}(OH)$. The sample is a finely crushed powder.

The high-pressure apparatus on wiggler 16.4 of the synchrotron radiation source at Daresbury Laboratory, U.K., is a 6/8 split-cylinder multi-anvil apparatus of the Walker design (Walker et al. 1990; Walker 1991). This "Walker cell" is mounted horizontally, so that the synchrotron beam passes through a hole in the aluminium end-plate, and through gaps between the steel wedges and tungsten carbide cubes before it reaches the ceramic octahedron containing the sample. The transmitted and diffracted beams exit through a similar set of gaps and holes. White-beam radiation is used, and a solid-state detector mounted at an angle 2θ typically around 5° is used to obtain an energy-dispersive diffraction pattern of the sample. Further details of the Walker cell and detector system are given in Clark (1996).

In the experiments on zoisite, tungsten carbide cubes with truncated-edge lengths of 12 mm were used. The sample assembly was comprised of a cast ceramic octahedron containing a cylindrical graphite furnace (o.d. = 6 mm, i.d. = 5 mm), inside which was a glass capsule containing the sample and NaCl pressure standard (o.d. = 5 mm, i.d. = 2.9 mm). Glass was used as the capsule material because it does not absorb or diffract the X-rays. Its potential reactivity with the sample does, however, limit its use to temperatures well below the maximum stability of the samples. Approximately 2 mm length of compressed sample was placed at one end of the glass capsule, with ≈1 mm of powdered NaCl below it. A Pt/Pt10Rh thermocouple was embedded in the capsule, with its tip in the sample. The glass capsule was positioned so that the sample was in the central hot spot of the furnace, the tip of the axial thermocouple just above the center of the sample and the NaCl below it.

Temperature gradients in the assembly were measured in an experiment using two thermocouples separated by 1.5 mm. At temperatures up to 1000 °C, the gradient was ≈10 °C/mm. By ensuring that the diffracting sample was within 1 mm of the thermocouple tip, an uncertainty on the temperature measurement of ±10 °C was assumed. Temperature was controlled to within ±1 °C, with no adjustment made for the effect of pressure on thermocouple emf.

With the small detector angle 2θ of 4.84° used here, the volume of material from which diffracted beam reaches the detector is ≈5 mm long in the beam direction and

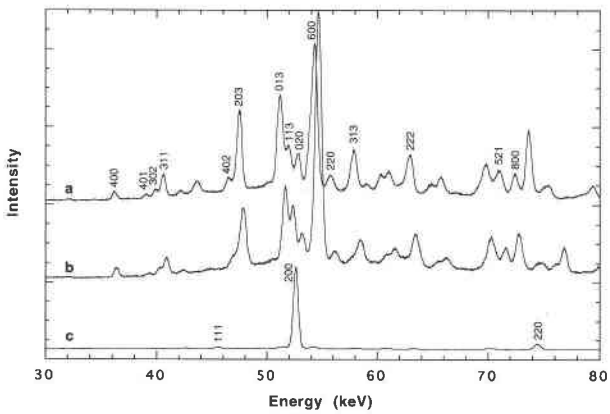

FIGURE 1. Energy-dispersive diffraction patterns of zoisite and NaCl in the Walker cell. Detector angle is 4.84° 2θ. (**a**). Zoisite at ambient pressure and temperature obtained at the end of the experiment. Zoisite peaks that can be followed through unambiguously to higher pressure and temperature are indexed. (**b**). Zoisite at 3500 kN (6.13 GPa), 800 °C. (**c**). NaCl at 1000 kN (0.80 GPa), 20 °C.

≈0.5 mm perpendicular to the beam. Therefore, with the press and detector correctly positioned with respect to the synchrotron beam it is possible to obtain a diffraction pattern comprised predominantly of sample peaks. Because the solid-state detector detects all energies simultaneously, a high-resolution diffraction pattern of the sample can usually be collected in 10–20 min. The useful range in energies obtainable with the multi-anvil press at Daresbury is from 30–100 keV, with the maximum intensity at approximately 40 keV. The detector angle was adjusted to ensure that as many useful sample diffraction peaks as possible are in this energy range and then determined by measuring the peak positions for a standard such as Si or NaCl.

A typical experimental procedure for conducting these high *P-T* volume measurements is to apply a sufficient load to the sample (equivalent to ≈1 GPa) to ensure that a good electrical circuit has been made and then to collect XRD patterns at a series of temperatures while maintaining this load. Power to the furnace is then turned off, the load is increased, and the heating cycle is repeated. For our experiments on zoisite, diffraction patterns were collected at each *P-T* point for 15 min. A typical low-pressure diffraction pattern is shown in Figure 1a. Peak positions were obtained by fitting Gaussian profiles to the diffraction data. Indexing the diffraction patterns was not straightforward, because there are potentially a lot of closely spaced zoisite peaks in the observed energy range. Therefore, observed peak positions were compared with expected positions (calculated using the program DRAGON v3.1, written by J.C. Cockcroft), cell parameters were refined by nonlinear least-squares using the program UnitCell (Holland and Redfern 1997), and then indexing was continuously checked as pressure and temperature were increased. As shown in Figure 1a, several peaks in the diffraction pattern were not used. Omissions were needed because a few sample peaks overlap with peaks from the ceramic pressure medium, whereas the indexing of others was ambiguous due to overlap of more than one zoisite peak. Up to 15 peaks were used in low *P-T* cell refinements. Figure 1b shows a high *P-T* diffraction pattern, in which most of the same peaks visible at low pressure and temperature are still identifiable. More peak overlap at high pressure and temperature reduced the number of indexable peaks in some diffraction patterns, to a minimum of eight.

At each *P-T* point for which a diffraction pattern was collected of the sample, one was also collected of the adjacent NaCl pressure standard after making a small adjustment to the press and detector positions to bring the NaCl into the diffracting position. A typical NaCl diffraction pattern is shown in Figure 1c. Although it contains small peaks from adjacent sample, three NaCl peaks are measurable. From each peak, the unit-cell edge was calculated and the pressure determined using the EOS of NaCl given by Decker (1971). We assumed that the temperature of the NaCl was the same as that of the zoisite, as measured by the thermocouple embedded in the sample. Pressures from the three NaCl peaks were averaged to give the values shown in Table 1. Sometimes sample peak overlap meant that the measured position of one NaCl peak produced a pressure significantly different from the others, in which case this peak's pressure was not included in the average. The uncertainties on pressure given in Table 1 are the standard deviation of the two or three measured pressures.

RESULTS

All of the unit-cell parameters determined here (Table 1) were collected on the same sample. Six heating cycles were completed at loads from 1000 to 3500 kN before a short circuit between the steel wedges in the Walker cell prevented further heating. The first measurement at each load was made with the heater switched off, but this was usually at greater than room temperature because the cell was still warm after the previous heating cycle. The difference from room temperature was not sufficient to justify taking up valuable synchrotron beamtime waiting for the press to cool down. Subsequent measurements were made at 200 °C steps upward from 200 °C. The highest temperature at each load was chosen to be well below the stability limit of zoisite at this pressure: 600 °C below ≈4 GPa, and 800 °C at higher pressure.

Table 1 also shows that pressure always increased as the sample expanded with temperature. This effect is illustrated in Figure 2, which shows all but the last two *P-T* points. The increase of >1 GPa as temperature is increased from room temperature to 600 °C at constant load is substantial, and shows that, in the multi-anvil apparatus, temperature cannot be ignored in any calibration of sample against oil pressure.

The two diffraction patterns collected during unloading showed that no irreversible changes to the sample had

TABLE 1. High *P-T* cell constants of zoisite

Load (kN)	*P* (GPa)	*T* (°C)	*a* (Å)	*b* (Å)	*c* (Å)	*V* (Å³)
1000	0.80(1)*	20	16.20(1)	5.562(4)	10.04(1)	905(1)
1000	1.12(2)*	200	16.20(2)	5.582(5)	10.00(2)	905(1)
1000	1.60(4)*	400	16.20(3)	5.570(2)	10.03(4)	905(4)
1000	1.64(6)*	600	16.25(3)	5.591(2)	10.04(4)	913(4)
1500	1.83(3)*	32	16.16(3)	5.55(1)	9.99(3)	896(3)
1500	2.21(8)*	200	16.16(3)	5.56(2)	10.00(4)	898(4)
1500	2.57(7)*	400	16.18(3)	5.55(1)	10.03(3)	901(3)
1500	2.86(2)*	600	16.20(3)	5.56(2)	10.04(4)	904(4)
2000	2.61(3)†	34	16.16(2)	5.54(1)	10.03(3)	897(3)
2000	2.97(2)†	200	16.15(3)	5.54(2)	10.00(4)	895(4)
2000	3.44(1)†	400	16.16(3)	5.55(2)	10.00(4)	897(4)
2000	3.67(1)†	600	16.18(3)	5.56(1)	10.02(3)	901(3)
2500	3.30(2)†	34	16.15(3)	5.53(2)	9.98(3)	891(3)
2500	3.68(1)†	200	16.14(3)	5.53(2)	9.96(4)	889(3)
2500	4.18(6)†	400	16.14(3)	5.53(2)	9.98(4)	891(3)
2500	4.49(6)†	600	16.16(3)	5.54(2)	10.00(4)	895(3)
3000	4.1(1)*	36	16.12(3)	5.52(2)	9.93(4)	885(3)
3000	4.6(1)*	200	16.13(3)	5.52(3)	9.97(4)	887(4)
3000	5.0(1)*	400	16.12(2)	5.53(2)	9.96(3)	888(3)
3000	5.4(1)*	600	16.13(2)	5.54(1)	9.98(2)	891(2)
3000	5.5(1)*	800	16.16(3)	5.53(1)	9.99(3)	894(3)
3500	4.4(1)†	21	16.11(2)	5.505(6)	9.92(2)	879(2)
3500	4.9(2)*	200	16.11(2)	5.509(7)	9.92(2)	881(2)
3500	5.3(2)*	400	16.11(1)	5.513(5)	9.93(2)	882(1)
3500	5.8(2)*	600	16.11(2)	5.516(5)	9.94(2)	884(2)
3500	6.1(1)*	800	16.14(2)	5.520(5)	9.96(2)	887(2)
4000‡	4.9(1)†	37	16.11(2)	5.501(7)	9.91(2)	878(2)
4500‡	5.5(2)*	30	16.08(1)	5.487(4)	9.89(1)	872(1)
5000‡	6.2(2)*	27	16.04(1)	5.480(5)	9.87(1)	867(1)
§ ‡	0.98(2)*	25	16.21(1)	5.554(4)	10.03(1)	903(1)
§ ‡	0.00	25	16.219(9)	5.566(3)	10.05(1)	907(1)

Note: Numbers in parentheses after pressures are the standard deviation on the last digit. Numbers in parentheses after cell parameters are 95% confidence limits on the last digit.

* Three NaCl peaks were used to obtain the pressure.

† Two NaCl peaks were used.

‡ Heating not possible due to short circuit.

§ During unloading.

occurred during pressurization and heating. The first diffraction pattern was collected when most of the load had been released, and the second on complete depressurization. The latter provided us with our only room *P-T* refinement of zoisite inside the Walker cell. The refined volume was slightly higher than a volume determined at room pressure and temperature outside the Walker cell. We have found similar differences for other samples, probably due to a slight movement in detector angle as the Walker cell is moved into position. This difference is not important in this study, as we are only interested in relative volumes as pressure and temperature are changed.

Zoisite compressibility at room temperature

The isothermal bulk modulus of a phase, K_T, and its pressure derivative, K', are commonly derived by fitting the Murnaghan equation to compressibility data:

$$V_{P,T}/V_{0,T} = [1 + K'/K_T \cdot P]^{-1/K'} \quad (1)$$

where $V_{P,T}$ is the unit-cell volume at pressure, P (in GPa), and temperature, T (in K), and $V_{0,T}$ is the volume at 0 GPa and temperature T. Measurements are usually made at room temperature (298 K). Equation 1 was fit to the

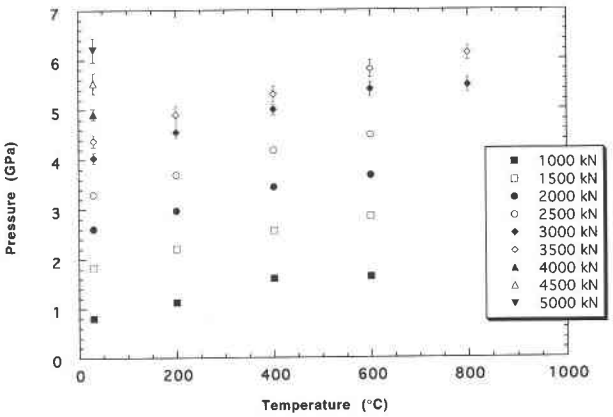

FIGURE 2. Variation of sample pressure with temperature and with load on the Walker cell. Sample pressure was measured from the internal NaCl standard. The legend shows the load in kilonewtons for each heating cycle. Errors on pressure are taken from Table 1.

close-to-room-temperature volume data in Table 1 (average temperature = 30 °C or 303 K) using a fixed value of K' (= 4). Fixing K' at 4 is a common procedure when data are few or scattered (e.g., Holland et al. 1996). From the least-squares fit (Fig. 3), K_{303} = 127(4) GPa, $V_{0,303}$ = 909.0(7) Å³ (numbers in parentheses are the standard deviation on the last digit). This value of $V_{0,303}$ was used to obtain $V_{P,303}/V_{0,303}$. Linear fits of the individual cell parameters relative to their values at 0 GPa (Fig. 3) gave compressibilities β_a = 0.0016(1), β_b = 0.0026(1), β_c = 0.0030(1) GPa⁻¹. Thus, the relative compressibility of the three axes is $c > b > a$. The bulk modulus of zoisite at 303 K is close to that obtained at room temperature by Comodi and Zanazzi (1997a) [102(7) GPa for an approx-

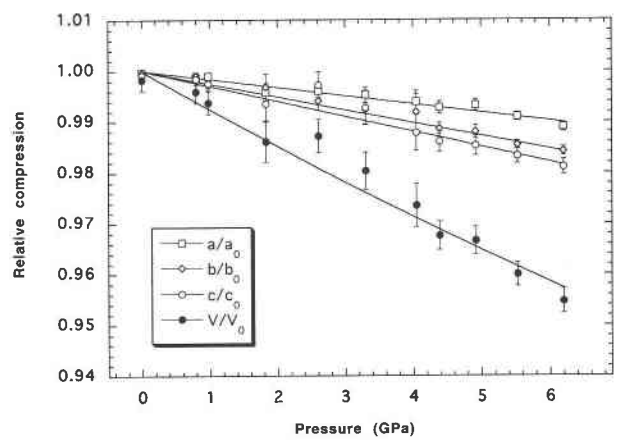

FIGURE 3. Compressibility of zoisite at ≈303 K. Error bars are 95% confidence limits on the cell refinements. Curve through volume data is the least-squares fit to the Murnaghan equation; the other lines are linear fits to the individual cell parameters. Data points are normalized to 0 GPa values obtained from the fits.

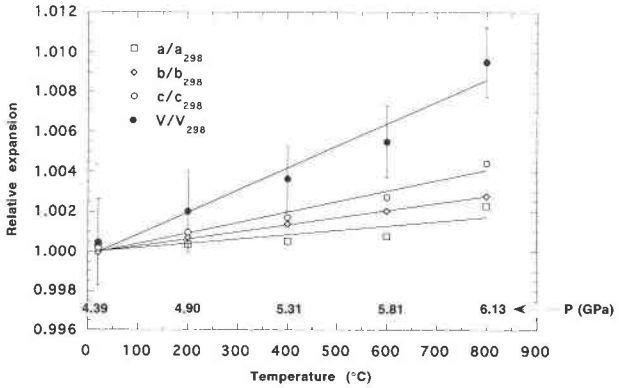

FIGURE 4. Thermal expansivity of zoisite at constant load (3500 kN). Error bars are 95% confidence limits on V/V_{298}. Equivalent error bars on the individual cell parameters would be approximately one-half the size of those on V/V_{298}. Pressures at each temperature are shown.

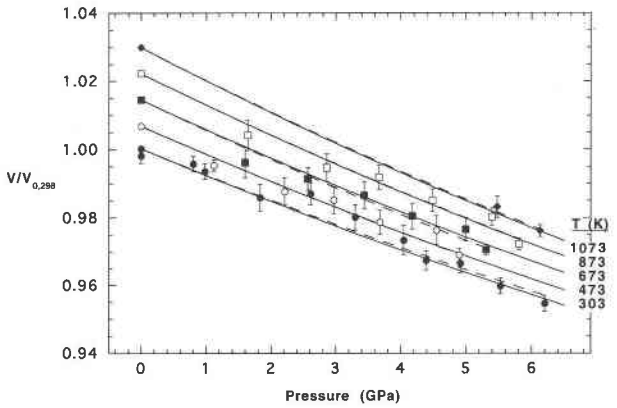

FIGURE 5. Zoisite volume data used to determine bulk modulus as a function of temperature. Error bars are 95% confidence limits on $V/V_{0,298}$. Points with no error bars are calculated from Equation 2. Dashed curves are Murnaghan fits to the data. Solid curves are model compressibilities (see text for further discussion).

imated $K' = 4.8$], but much lower than that obtained by Holland et al. (1996) [279(9) GPa for $K' = 4$].

Thermal expansivity of zoisite

Because sample pressure increases significantly during heating, no volume measurements were made at low pressure and high temperature, and so we cannot use our data to determine the thermal expansivity of zoisite at ambient pressure. Therefore, we used the recent thermal expansivity measurements of Pawley et al. (1996). Volumes measured up to 750 °C were linear in temperature, with small errors. The data were fit by the equation

$$V_{0,T}/V_{0,298} = 1 + \alpha(T - 298), \qquad (2)$$

giving a constant value for the coefficient of thermal expansion, α, of $3.86(5) \times 10^{-5}$ K^{-1}, which is used below in the derivation of $\partial K_T/\partial T$. Although we could not determine thermal expansivity at ambient pressure, or at a fixed higher pressure (due to the temperature-dependence of pressure), we can usefully observe the relative expansion of the three cell axes as temperature is increased at constant load. Figure 4 shows the data for a load of 3500 kN, normalized to 298 K values obtained from linear fits of the data. For clarity, the only error bars shown are those on V/V_{298}. Values of pressure are given below the data points. Figure 4 shows that the relative expansivity of the three axes is $c > b > a$.

Effect of pressure on thermal expansivity

The main components of a mineral's equation of state, the compressibility at ambient temperature, and thermal expansivity at ambient pressure, are described above. However, to describe values at high pressure and high temperature it is necessary to know either the effect of temperature on compressibility or the effect of pressure on thermal expansivity. In our experiments it was not practical to hold pressure constant while the sample was heated, since we could only determine pressure after the diffraction pattern was collected. Therefore we could only measure compressibility as a function of temperature, from which we can determine the temperature derivative of the bulk modulus, $\partial K_T/\partial T$. We therefore fit Equation 1 to the volume data at each measurement temperature. However, without any low-pressure, high-temperature measurements, we did not have enough data points to determine the bulk modulus with sufficient accuracy at high temperature. We therefore also calculated $V_{0,T}$ at 200, 400, 600, and 800 °C from Equation 2, and forced the fitted curves to go through these points. Figure 5 shows all of the data used in the calculations. Points with error bars are our data; points with no error bars are calculated from Equation 2. All data are given as $V/V_{0,298}$. For our multi-anvil data, $V_{0,298}$ was calculated from $V_{0,303}$ obtained from the Murnaghan fit to the low-temperature data, using Equation 2. By fitting the Murnaghan equation to each of the five sets of isothermal data (Fig. 5), we obtained the following values of K: $K_{303} = 127(4)$ GPa (also shown in Fig. 3), $K_{473} = 119(5)$ GPa, $K_{673} = 111(4)$ GPa, $K_{873} = 109(3)$ GPa, $K_{1073} = 103(3)$ GPa. The bulk modulus clearly decreases with temperature. Assuming a linear relationship, a least-squares fit of the data gives $K_{298} = 125(3)$ GPa, $\partial K_T/\partial T = -0.029(6)$ GPa K^{-1} (Fig. 6). We now have enough information to be able to calculate $V_{P,T}/V_{0,298}$ for any pressure and temperature within the range of our experiments. Combining Equations 1 and 2 gives

$$V_{P,T}/V_{0,298} = [1 + \alpha(T - 298)][1 + K'/K_T \cdot P]^{-1/K'}$$

$$\text{where } K_T = K_{298} + \partial K_T/\partial T \cdot T.$$

Using $\alpha = 3.86 \times 10^{-5}$ K^{-1}, $K_{298} = 125$ GPa, $\partial K_T/\partial T = -0.029$ GPa K^{-1}, and assuming $K' = 4$ at all temperatures, we have constructed model compressibility curves at different temperatures (Fig. 5).

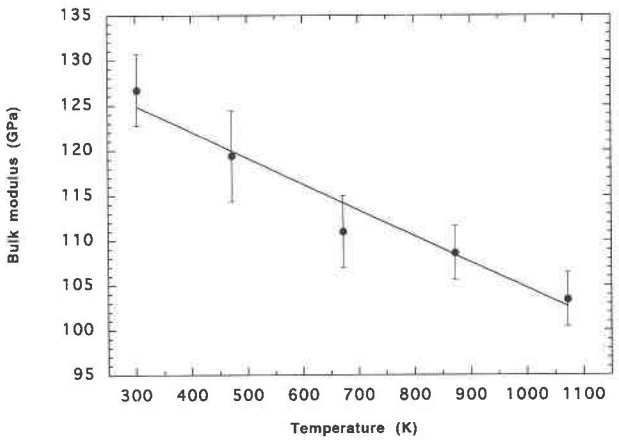

FIGURE 6. Bulk modulus of zoisite as a function of temperature. Bulk moduli are obtained from the Murnaghan fits in Figure 5. The best-fit straight line has the equation $K_T = 125(3) - 0.029(6)\ (T - 298)$ GPa.

DISCUSSION

Structural behavior of zoisite at elevated pressure and temperature

The structure of zoisite was refined by Dollase (1968). It contains chains of edge-sharing AlO_6 octahedra running parallel to **y**. In these chains, M1 octahedra share three edges with neighboring octahedra, and M2 octahedra share two edges. The chains are cross-linked by corner-sharing Si_2O_7 tetrahedral pairs and single SiO_4 tetrahedra parallel to **z.** Ca occupies large irregular cavities between the chains. H is bonded to an O of the octahedral chain and also may be hydrogen-bonded to an O of the adjacent chain (Dollase 1968). Our results show that cell parameters and volume of zoisite vary smoothly as pressure and temperature are increased. There is only a small difference in behavior of the three unit-cell parameters. The *c* parameter has the greatest compressibility and expansivity, while the *a* parameter has the least. This is the same relative behavior as observed for thermal expansivity by Pawley et al. (1996), except in that study the *a* parameter showed almost no expansion. Our relative compressibilities are also the same as those observed for both zoisite and clinozoisite by Comodi and Zanazzi (1997a). In describing the compressibility of clinozoisite, they point out that there is less separation of adjacent "building blocks" of octahedra along **x** than along **z**, and so there is less compression along **x**. A similar arrangement of building blocks exists in zoisite, allowing its structure to take up more compression along **z** than along **x**. In common with most minerals, our data demonstrate that zoisite shows the same relative behavior during expansion as during compression.

Comparison of compressibility with previous studies

Two recent studies have determined the compressibility of zoisite, with markedly different results. Holland et al. (1996) compressed a powdered sample (the same as in this study) in a diamond-anvil cell, and used synchrotron radiation to measure its volume. They obtained K_{298} = 279 GPa (for $K' = 4$). Comodi and Zanazzi (1997a) used single-crystal XRD and obtained K_{298} = 102 GPa (for $K' = 4.8$). There are no obvious reasons to suspect the quality of either data set, but comparison of the Holland et al. (1996) data with other results suggests that it is in error. The reasons for suspecting this are, first, that the compressibility of zoisite was significantly different from the compressibility of clinozoisite obtained in the same study (K_{298} = 154 GPa), which is surprising given their similar structures; and second, that the relative compression of the three axes was different from the relative expansion obtained by Pawley et al. (1996) and also obtained in this study. The compressibility data obtained in this study (K_{298} = 125 GPa for $K' = 4$) are in much better agreement with the data of Comodi and Zanazzi (1997a) than with the data of Holland et al. (1996), and so it is clear that there was a problem with the latter measurements. We have therefore rechecked the indexing of the diffraction patterns obtained by Holland et al. (1996). After a small amount of re-indexing, the resulting cell refinements are not very different from the published values, but there now appears to be very little change in volume at low pressures, increasing to a more reasonable compressibility at high pressures. It would seem, therefore, that the initial compression being measured by the NaCl pressure standard is not being experienced by the powdered zoisite.

$\partial K_T/\partial T$

From our data we have obtained $\partial K_T/\partial T = -0.029(6)$ GPa K^{-1}. We assumed that $\partial K_T/\partial T$ is constant, because it is evident from previous data on other high-pressure phases that K_T is approximately linear in temperature (e.g., Anderson et al. 1992). Our data can be used to estimate the Anderson-Gruneisen parameter for zoisite at 298 K, δ_{298}, given by the relationship

$$\delta T = -(1/\alpha K_T)\cdot(\partial K_T/\partial T)_P.$$

From Pawley et al. (1996), $\alpha = 3.86 \times 10^{-5}$ K^{-1}, and from this study, K_{298} = 125 GPa and $\partial K_T/\partial T = -0.029$ GPa K^{-1}. Therefore $\delta_{298} = 6.0$. This value is similar to that obtained for other high-pressure phases (e.g., Anderson et al. 1992), and supports the use in Holland et al. (1996) of an average value of $\delta_{298} = 7.0$ to calculate $\partial K_T/\partial T$ for all minerals in the revised thermodynamic data set and computer program THERMOCALC (Holland and Powell 1990, revisions described in Holland et al. 1996).

Zoisite stability in the Earth

Quantitative calculations of zoisite reactions using our new volume data are beyond the scope of this paper, due to the considerable amount of other thermodynamic data involved. However, we can make some qualitative observations. For example, Holland et al. (1996) calculated that the maximum pressure stability of zoisite, through the reaction zoisite = grossular + kyanite + coesite + H_2O,

occurs at pressures ≈2.5 GPa below those observed experimentally (Schmidt and Poli 1994). At that time it was not possible to explain this pressure difference, but it is now clear that with a much lower bulk modulus, and hence higher compressibility, the calculated reaction pressures are substantially increased, bringing them into line with the experimental pressures, and confirming the high-pressure stability of zoisite in the Earth. Our bulk modulus is ≈25% higher than measured by Comodi and Zanazzi (1997a). We used $K' = 4$ in our calculation of K_{298}, whereas those authors used $K' = 4.8$. Recalculating our data using $K' = 4.8$ results in a decrease in K_{298} of 2%. This value is still significantly higher than that of Comodi and Zanazzi (1997a), and so calculations using their data tend to increase the pressure stability of zoisite in comparison to calculations using our data.

Our complete data set can be used to determine the behavior of zoisite volume along different geothermal gradients in the Earth. We used the model curves in Figure 5 to extract the *P/T* gradient at which $V/V_0 = 1$. Between 0 and 3 GPa, this averages out at approximately 240 K/GPa, equivalent to 42 bar/K, or 8 °C/km in the Earth. Under a typical continental shield geotherm of ≈10 °C/km, zoisite's volume therefore increases with depth, but under typical subduction zone geotherms, which are <8 °C/km, its volume decreases with depth. For example, *P-T* paths presented by Peacock et al. (1994) for the top of subducting slab have gradients of ≈100 K/GPa between 2 and 5 GPa, equivalent to ≈3 °C/km. Therefore in a typical subduction zone, zoisite becomes more dense as subduction proceeds, helping to stabilize it to high pressures.

Acknowledgments

A.R.P. acknowledges the support of Daresbury grant 28445, and N.C. the support of NERC studentship GT4/95/223/E. We thank Ray Jones for his assistance in sample preparation and press operation, and an anonymous reviewer for helpful comments on the manuscript.

References cited

Anderson, O.L., Isaak, D., and Oda, H. (1992) High-temperature elastic constant data on minerals relevant to geophysics. Reviews of Geophysics, 30, 57–90.

Burnham, C.W., Holloway, J.R., and Davis, N.F. (1969) The specific volume of water in the range 1000 to 8900 bars, 20° to 900°C. American Journal of Science, 256-A, 70–95.

Clark, S.M. (1996) A new energy dispersive powder diffraction facility at the SRS. Nuclear Instruments and Methods in Physical Research, A381, 161–168.

Comodi, P. and Zanazzi, P.F. (1996) Effects of temperature and pressure on the structure of lawsonite. American Mineralogist, 81, 833–841.

——— (1997a) The pressure behavior of clinozoisite and zoisite: An X-ray diffraction study. American Mineralogist, 82, 61–68.

——— (1997b) Pressure dependence of structural parameters of paragonite. Physics and Chemistry of Minerals, 24, 274–280.

Decker, D.L. (1971) High-pressure equation of state for NaCl, KCl and CsCl. Journal of Applied Physics, 42, 3239–3244.

Dollase, W.A. (1968) Refinement and comparison of the structures of zoisite and clinozoisite. American Mineralogist, 53, 1882–1898.

Faust, J. and Knittle, E. (1994) Static compression of chondrodite: Implications for water in the upper mantle. Geophysical Research Letters, 21, 1935–1938.

Franz, G. and Selverstone, J. (1992) An empirical phase diagram for the clinozoisite-zoisite transformation in the system $Ca_2Al_3Si_3O_{12}(OH)$-$Ca_2Al_2Fe^{3+}Si_3O_{12}(OH)$. American Mineralogist, 77, 631–642.

Holland, T.J.B. (1979) High water activities in the generation of high pressure kyanite eclogites of the Tauern Window, Austria. Journal of Geology, 87, 1–27.

Holland, T.J.B. and Powell, R. (1990) An enlarged and updated internally consistent thermodynamic dataset with uncertainties and correlations: the system K_2O-Na_2O-CaO-MgO-MnO-FeO-Fe_2O_3-Al_2O_3-TiO_2-SiO_2-C-H_2-O_2. Journal of Metamorphic Geology, 8, 89–124.

Holland, T.J.B. and Redfern, S.A.T. (1997) Unit cell refinement from powder diffraction data: the use of regression diagnostics. Mineralogical Magazine, 61, 65–77.

Holland, T.J.B., Redfern, S.A.T., and Pawley, A.R. (1996) Volume behavior of hydrous minerals at high pressure and temperature: II. Compressibilities of lawsonite, zoisite, clinozoisite, and epidote. American Mineralogist, 81, 341–348.

Johnson, M.C. and Walker, D. (1993) Brucite [$Mg(OH)_2$] dehydration and the molar volume of H_2O to 15 GPa. American Mineralogist, 78, 271–284.

Libowitzky, E. and Armbruster, T. (1995) Low-temperature phase transitions and the role of hydrogen bonds in lawsonite. American Mineralogist, 80, 1277–1285.

Martinez, I., Zhang, J., and Reeder, R.J. (1996) In situ X-ray diffraction of aragonite and dolomite at high pressure and high temperature: Evidence for dolomite breakdown to aragonite and magnesite. American Mineralogist, 81, 611–624.

Meng, Y., Weidner, D.J., Gwanmesia, G.D., Liebermann, R.C., Vaughan, M.T., Wang, Y., Leinenweber, K., Pacalo, R.E., Yeganehhaeri, A., and Zhao, Y. (1993) In-Situ High *P-T* X-ray-diffraction studies on 3 polymorphs (alpha, beta, gamma) of Mg_2SiO_4. Journal of Geophysical Research, 98, 22199–22207.

Pawley, A.R. (1994) The pressure and temperature stability limits of lawsonite: Implications for H_2O recycling in subduction zones. Contributions to Mineralogy and Petrology, 118, 99–108.

Pawley, A.R. and Wood, B.J. (1995) The high-pressure stability of talc and 10 Å phase: Potential storage sites for H_2O in subduction zones. American Mineralogist, 80, 998–1003.

Pawley, A.R., Redfern, S.A.T., and Wood, B.J. (1995) Thermal expansivities and compressibilities of hydrous phases in the system MgO-SiO_2-H_2O: talc, phase A and 10Å phase. Contributions to Mineralogy and Petrology, 122, 301–307.

Pawley, A.R., Redfern, S.A.T., and Holland, T.J.B. (1996) Volume behavior of hydrous minerals at high pressure and temperature: I. Thermal expansion of lawsonite, zoisite, clinozoisite, and diaspore. American Mineralogist, 81, 335–340.

Peacock, S.M., Rushmer, T., and Thompson, A.B. (1994) Partial melting of subducting oceanic crust. Earth and Planetary Science Letters, 121, 227–244.

Redfern, S.A.T. and Wood, B.J. (1992) Thermal expansion of brucite, $Mg(OH)_2$. American Mineralogist, 77, 1129–1132.

Schmidt, M.W. and Poli, S. (1994) The stability of lawsonite and zoisite at high pressures: Experiments in CASH to 92 kbar and implications for the presence of hydrous phases in subducted lithosphere. Earth and Planetary Science Letters, 124, 105–118.

Ulmer, P. and Trommsdorff, V. (1995) Serpentine stability to mantle depths and subduction-related magmatism. Science, 268, 858–861.

Walker, D. (1991) Lubrication, gasketing, and precision in multianvil experiments. American Mineralogist, 76, 1092–1100.

Walker, D., Carpenter, M.A., and Hitch, C.M. (1990) Some simplifications to multianvil devices for high pressure experiments. American Mineralogist, 75, 1020–1028.

Xu, J., Hu, J., Ming, L., Huang, E., and Xie, H. (1994) The compression of diaspore, AlO(OH) at room temperature up to 27 GPa. Geophysical Research Letters, 21, 161–164.

Manuscript received November 7, 1997
Manuscript accepted April 14, 1998
Paper handled by Simon A.T. Redfern